Effect of multiple shaking events on cone penetration resistances in saturated sand

Kathleen M. Darby, Ross W. Boulanger, Jason T. DeJong
Department of Civil and Environmental Engineering- University of CA, Davis, CA, United States

ABSTRACT
This paper examines the effect of shaking history on cone penetration resistances. A pair of saturated Ottawa sand models, with initial relative densities of 25-30% and 75-80%, were subjected to repeated shaking events using the UC Davis 9-m radius geotechnical centrifuge. The initially loose model was subjected to 24 shaking events and the initially dense model was subjected to 17 shaking events. Multiple cone soundings were performed during each test to track changes in penetration resistance as shaking progressed; eight cone soundings were performed in the initially loose model and eleven cone soundings were performed in the initially dense model. Cone penetration resistances were found to increase after repeated shaking in both the initially loose and initially dense models. Changes in relative density estimated from cone penetration correlations tracked reasonably well with changes in relative density estimated from settlements.

1 INTRODUCTION

The effects of prior earthquake loading, and particularly prior liquefaction events, on the cone penetration resistance and cyclic strength of soil has long been of interest to interpretation of field case histories. Many of the case histories in liquefaction triggering databases only have post-event cone penetration test (CPT) data, which raises the question of how well these data represent pre-event conditions.

Recent experimental studies have begun to provide data on the influence of cyclic loading on penetration resistances or other strength indices, such as relative density (D_R) or shear wave velocity (V_s). Sharp et al. (2010) found cone penetration resistance increased more than expected for the observed increase in D_R computed from surface settlements in an unsaturated Nevada sand model subjected to pre-shaking. El-Sekelly et al. (2015, 2016) investigated the effect of repeated sequences of low level shaking events separated by two progressively stronger shaking events capable of triggering liquefaction in a saturated silty sand model. They found that the occurrence of extensive liquefaction could temporarily decrease liquefaction resistance for a subsequent event (based on differences in excess pore pressure generation), but that multiple events would ultimately increase the liquefaction resistance. They observed V_s increases of less than 10% for D_R increasing from 38 to 50%. A large scale shaking table test as part of the same experimental study found the cone penetration resistance to be significantly more sensitive than V_s to shaking history (Dobry and Abdoun 2016). Darby et al. (2016) conducted a set of 1-m radius centrifuge tests with mini cone penetration tests to investigate the effects of multiple liquefaction events on cyclic resistance ratio (CRR) and penetration resistances in saturated Ottawa F-65 sand models. Their initial results suggested that the correlation of CRR with cone penetration resistance in clean sand is not significantly dependent on shaking history, at least for the range of conditions examined in their tests.

Other research studies have provided data on the effect of cyclic loading on liquefaction resistance. Ha et al. (2011) performed a set of 1-g shaking table tests and observed an initial decrease followed by an increase in the liquefaction resistance of sands after multiple liquefaction events. Parra Bastidas et al. (2016) performed cyclic direct simple shear (DSS) tests on saturated Ottawa F-65 sand and observed a significant increase in cyclic strength after being subjected to multiple liquefaction/cyclic straining events followed by reconsolidation phases. Similar increases in cyclic strength following repeated shearing and reconsolidation phases were observed in cyclic DSS tests on non- and low plasticity silt (Price et al. 2017).

This paper examines the effects of repeated shaking events on cone penetration resistances measured in saturated sand models on a 9-m radius geotechnical centrifuge. The results presented in this paper are part of a larger research program investigating the simultaneous effect(s) of shaking history on cone penetration and liquefaction resistance, and the interactions between the two. This paper describes how cone penetration resistances changed over the course of repeated shaking events and the associated generation/non-generation of large excess pore pressures and strains. The centrifuge cone penetration testing procedures, representative penetration resistance profiles, and the influence of multiple shaking events are described. Future use and implications for practice are discussed.

2 CENTRIFUGE MODEL AND CONE TESTING

The two centrifuge models were constructed in a flexible shear beam container and tested on the 9-m radius geotechnical centrifuge at the University of California at Davis. Both models were level ground soil profiles (cross-section in Figure 1) comprised of an 18-cm-thick layer of dense Monterrey sand (initial D_R=85%) overlain by a 28-cm-thick layer of Ottawa sand (initial D_R of 25-30% in Test 1; initial D_R of 75-80% in Test 2). The sands were placed by dry pluviation in a series of lifts, with lift thicknesses of 6 cm for the Monterrey sand and 4 cm for the Ottawa sand. The model was saturated with methylcellulose with a viscosity of 20 cSt. The centrifuge tests were performed at a centrifugal acceleration of 40 g. Results are scaled using

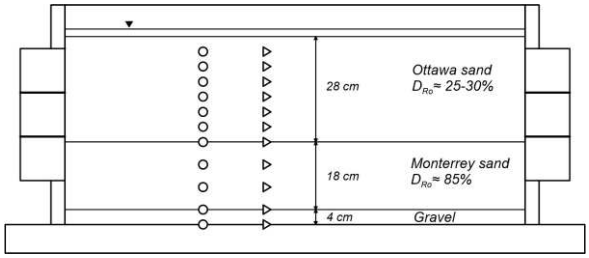

Figure 1. Cross section for Test 1. Dimensions in model units

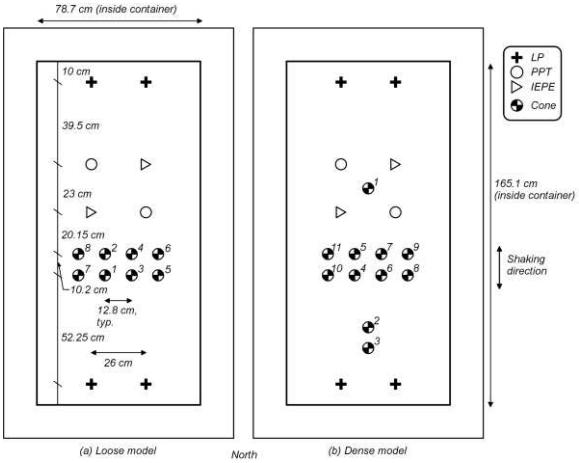

Figure 2. Plan view showing locations of cone soundings in the initially (a) loose and, (b) dense models. Dimensions in model units.

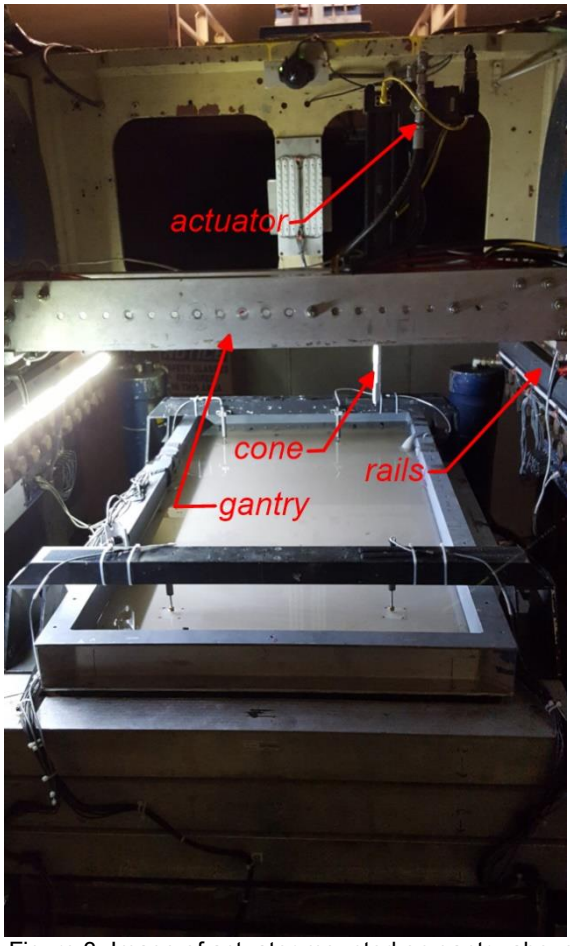

Figure 3. Image of actuator mounted on gantry above the model container.

standard scaling laws and presented in prototype units unless otherwise noted.

Plan views for the initially loose model (Test 1) and initially dense model (Test 2) are shown in Figures 2a and 2b, respectively. Pore pressure transducers (PPTs) and accelerometers (ACCs) were placed in vertical arrays in both models at the locations shown in Figure 1. The locations and sequence of cone penetration tests are also indicated on these figures.

Cone penetration tests were performed using an actuator mounted on a gantry that is supported on bearing rails and spans over the model, as shown by the photograph in Figure 3. Before spinning the centrifuge, the actuator can be manually repositioned on the gantry and the gantry can be manually repositioned along the bearing rails. In addition, the gantry is connected to the bearing rails through pneumatic actuators that enable the gantry to be moved a distance of 100 mm (model scale) while the centrifuge is spinning. This configuration allows for two cone penetration tests to be performed while the centrifuge is spinning, after which the centrifuge must be spun down and the actuator/gantry repositioned before additional tests can be performed. The cone penetrometer has a 6 mm diameter (model scale) and was pushed 300 mm (model scale) at 1 cm/sec in these tests. The 6 mm diameter is 30 times the median grain diameter of the Ottawa sand used in the present tests, which suggests scaling effects on cone penetration resistance should be small (Bolton et al. 1999).

The initially loose model was subjected to 24 shaking events, each consisting of 15 uniform sinusoidal cycles at a 1 Hz frequency. The peak base acceleration (PBA) progressively increased from about 0.03 g in the first event to about 0.2 g in the sixth event, and then this sequence of six events was repeated an additional three times. The excess pore pressure ratio (r_u), which is the ratio of excess pore pressure (u_e) to initial vertical effective stress (σ'_{vo}), was determined at each PPT location. The PBA and peak r_u values for each event are plotted versus event number in Figure 4; the symbols are plotted versus PBA on the left y-axis, with the symbol shape identifying depth in the soil profile (3.7, 5.6, 6.7 m) and the symbol color identifying the peak r_u value (red indicates $r_u \geq 95\%$, yellow indicates r_u between 70-95%, and open points indicate $r_u < 70\%$). The average volumetric strain, depicted in grey, is calculated as the average surface settlement divided by the initial thickness of the Ottawa sand layer, and is plotted against the right y-axis for each shaking event. Each shaking event was separated a much greater amount of time than was required for full dissipation of excess pore water pressures.

The initially dense model was subjected to 17 shaking events, also all consisting of 15 uniform sinusoidal cycles

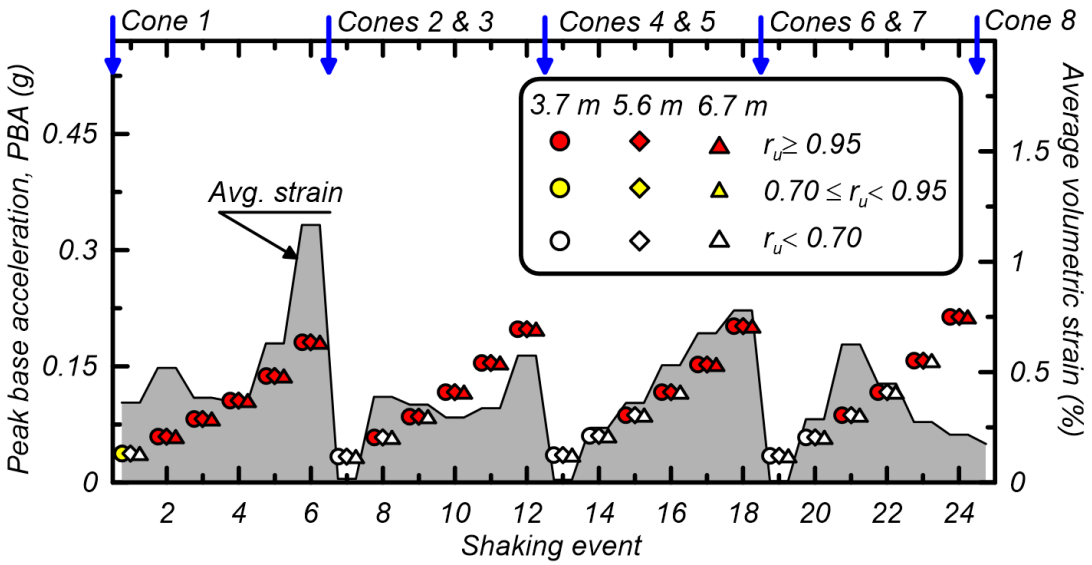

Figure 4. Test timeline of cone soundings, input accelerations, and generation of excess pore pressures and strains for the initially loose model.

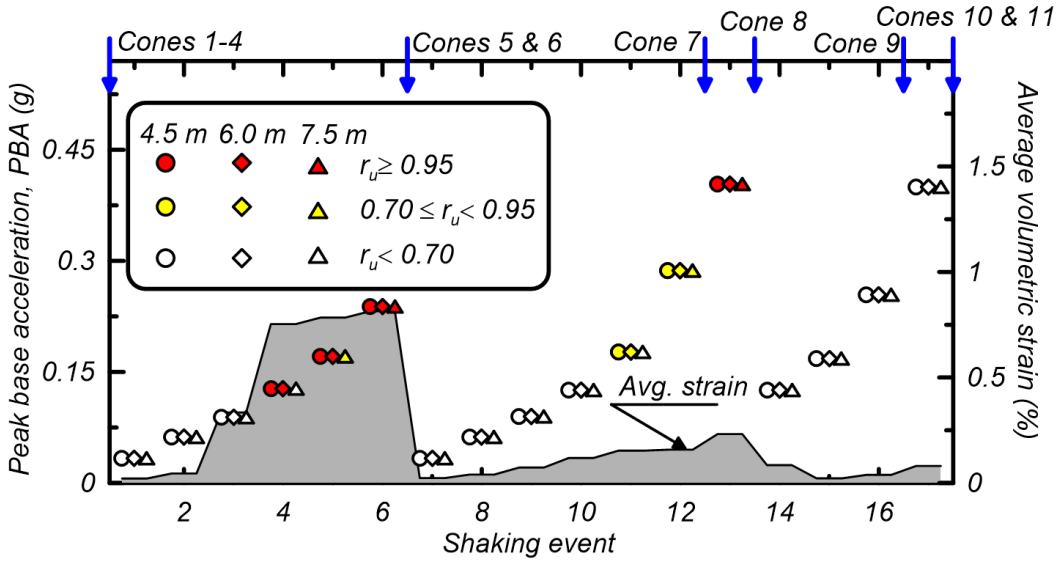

Figure 5. Test timeline of cone soundings, input accelerations, and generation of excess pore pressures and strains for the initially dense model.

at 1 Hz frequency. The PBA, peak r_u, and volumetric strain for each shaking event are plotted versus event number in Figure 5 using the same format described above for the initially loose test.

Cones were pushed between select shaking events for each model, with the timing of each cone sounding indicated by the blue arrows at the tops of Figures 4 and 5. For the initially loose model, one cone was pushed before any shaking (cone 1), two cones were pushed after each of the sixth (cones 2 & 3), twelfth (cones 4 & 5) and eighteenth (cones 6 & 7) shaking events, and one cone was pushed after all 24 shaking events (cone 8). For the initially dense model, four cones were pushed before any shaking (cones 1 to 4), two after the sixth shaking event (cones 5 & 6), one after each of the twelfth (cone 7), thirteenth (cone 8), and sixteenth (cone 9) shaking events, and two after all 17 shaking events (cones 10 & 11). The plan locations for each cone and their sequence are shown in Figure 2. The 100 mm (model scale) spacing between the cones pushed during the same centrifuge spin corresponds to 17 cone diameters, which is considered sufficient spacing to minimize their influence on each other. The positions and timing of the different cones provide data to evaluate spatial uniformity within the models before and after shaking, as well as the evolution of penetration resistance profiles over the course of the imposed shaking histories.

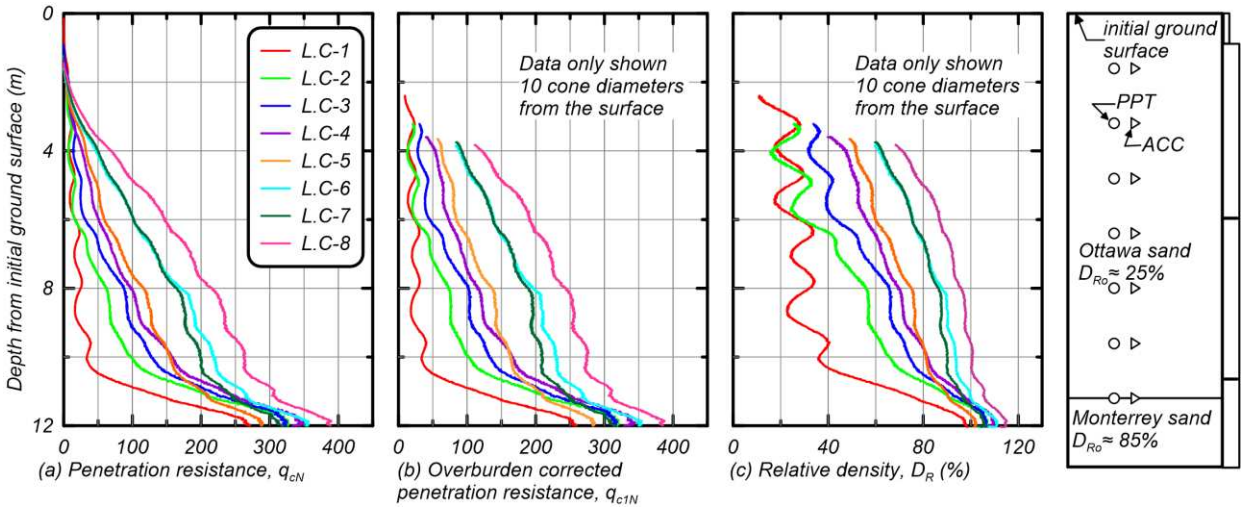

Figure 6. Profiles of (a) penetration resistance, (b) overburden corrected penetration resistance, and (c) relative density for all eight cone soundings in the initially loose model.

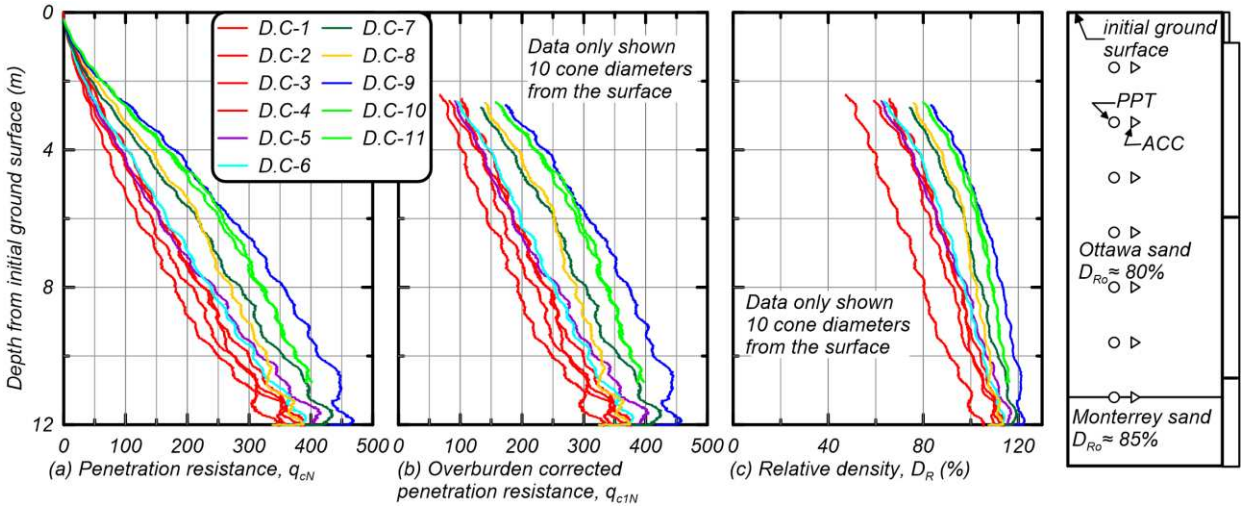

Figure 7. Profiles of (a) penetration resistance, (b) overburden corrected penetration resistance, and (c) relative density for all eleven cone soundings in the initially dense model.

3 CONE PENETRATION RESULTS

The measured penetration resistance ($q_{cN} = q_c/P_a$, where P_a = atmospheric pressure) from all the cone penetration soundings are plotted versus depth in Figure 6a for the initially loose model and Figure 7a for the initially dense model. Cones pushed in the initially loose model are identified by the initials L.C followed by the order of the cone push in the model; a similar naming convention is followed for cones pushed in the dense model. For the initially loose model, the cone prior to any shaking (L.C-1) gave q_{cN} ranging from about 8-40 between depths of 4 and 10 m, with q_{cN} increasing with depth as expected. This first q_{cN} profile has cyclical fluctuations with depth that correspond to the lift thicknesses, thus indicating slight variations in density across each lift. The q_{cN} values for subsequent cones (L.C-2 through 8) show progressive increases at all depths due to the shaking events, with the last cone giving q_{cN} values ranging from 70-260 between depths of 4 and 10 m. For the initially dense model, the cones prior to any shaking (D.C-1 through 4) gave q_{cN} ranging from about 70-270 between depths of 4 and 10 m. This first q_{cN} profile varies more smoothly with depth, indicating more uniform density across each lift than was obtained for the initially loose model. The q_{cN} values for subsequent cones (D.C-5 through 11) show progressive increases at all depths due to shaking events, with the last cone giving q_{cN} values ranging from 164-374 between depths of 4 and 10 m.

The cone penetration measurement is generally influenced by soils within about 10 to 30 cone diameters around the cone tip, with the degree of influence depending on the contrast in soil properties within the zone of physical influence. Ten cone diameters corresponds to a depth interval of 2.4 m (60 mm model scale) in the current tests.

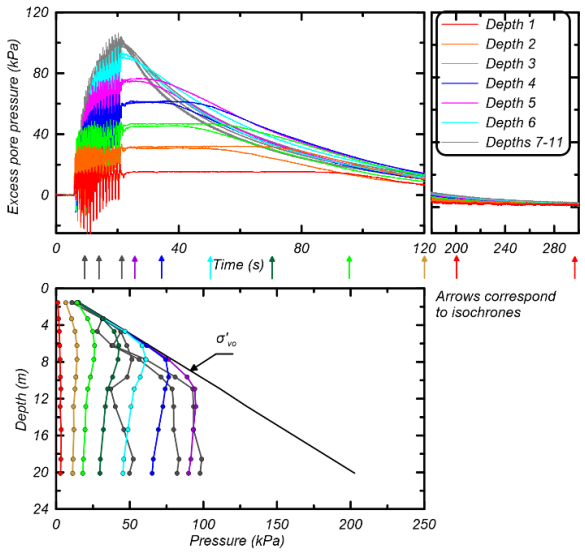

Figure 8. Excess pore pressure generation and dissipation time histories and isochrones depicting bottom up consolidation after Event 6 on the initially dense model.

The measured q_{cN} profiles in the initially loose model (Figure 6a) transition from low values in the loose sand layer to high values in the underlying dense Monterey sand layer over a distance of about 8.3 cone diameters (2 m) from a depth of about 10.2 m to just over 12 m. The cone senses the dense sand layer about 4 cone diameters (0.96 m) before reaching it (i.e. from 10.2 m to the layer interface at 11.2 m), and then appears to develop a nearly full representative resistance after another 4 cone diameters of penetration (i.e. from the layer interface to about 12 m or just past 12 m). The cones did not penetrate much further than 12 m into the dense Monterey sand layer so the development distance was likely a bit greater than the sensing distance. Overall, these profiles suggest that the q_{cN} in the Ottawa sand are influenced by the Monterey sand layer within a sensing distance of about 4 cone diameters.

The near-surface q_{cN} are similarly influenced by their proximity to the free ground surface. The development distance for q_{cN} below a ground surface is likely to be significantly greater than the 4 or 5 cone diameters at a loose sand to dense sand interface. For the present study, the q_{cN} in the Ottawa sand are assumed to be influenced by the ground surface to a depth of 10 cone diameters (i.e. 2.4 m prototype scale), although this development distance is more uncertain.

Overburden corrected penetration resistances, $q_{c1N} = C_N \cdot q_{cN}$, were computed using the overburden correction factor (C_N) relationship by Idriss and Boulanger (2008). Profiles of q_{c1N} are plotted in Figure 6b for the initially loose model and Figure 7b for the initially dense model. The q_{c1N} are not plotted within the zones influenced by the ground surface, as discussed above. The q_{c1N} values prior to any shaking (L.C-1 and D.C-1-4) tend to increase with depth in both models, which suggests that the D_R is also initially increasing with depth or the overburden correction is not fully removing the effects of overburden stress. The q_{c1N} in both models tend to increase more rapidly with depth after multiple shaking events, which suggests the models progressively densify more quickly at the larger depths.

Profiles of D_R were estimated from the q_{c1N} profiles using the relationship:

$$D_R = 0.465\left(\frac{q_{c1N}}{C_1}\right)^{0.264} - C_2 \qquad [1]$$

This equation is a modified form of the q_{c1N}-D_R relationship presented by Idriss and Boulanger (2008) with the constants, C_1 and C_2 calibrated for Ottawa sand. Based on data from three 9-m radius centrifuge tests, the values for C_1 and C_2 were estimated to be 3.086 and 0.514, respectively. The computed D_R values are plotted versus depth in Figure 6c for the initially loose model and Figure 7c for the initially dense model. For the initially loose model, the profiles of D_R indicate that densification of the Ottawa sand initiates at the base and progressively moves upward through the sand layer. After all shaking events, the lower half of the Ottawa sand layer has reached D_R of 90-100%, whereas the upper half has not yet become as dense. For the initially dense sand model, the lower half of the Ottawa sand layer increased from D_R of about 84-97% before shaking to about 105-110% after all shaking events, whereas the upper half increases from D_R of about 60-80% to about 80-100%. Thus, the densification caused the D_R to become more uniformly dense throughout the profile of the initially dense sand model.

The above patterns of densification can be understood by examining pore pressure dissipation behavior after the different shaking events. For example, excess pore pressure time series and isochrones for the thirteenth shaking event in the dense model are shown in Figure 8; this event generated high excess pore pressure throughout the Ottawa sand layer. The sand layer consolidates from the bottom up, indicating upward flow of pore water during and after shaking, as expected. This upward flow results in a greater rate of densification near the bottom of the loose sand layer, and conceptually may cause little densification or possibly even loosening near the ground surface. For the initially dense model, shaking events with smaller PBA only trigger high excess pore pressures in the upper portions of the Ottawa sand layer, such that the depth interval with the greatest rate of densification moves higher in the soil profile.

The D_R values estimated from the cone penetration data were checked with values estimated based on measured surface settlements. For the initially loose model, the cumulative surface settlement was 1.12 m (28 mm model scale) after all shaking events, which is an average vertical strain of 10% over the 10.2 m (0.28 m model scale) thick layer of Ottawa sand. This strain would produce an average increase in D_R from 25 to 85%, given the e_{max} = 0.83 and e_{min} = 0.51 values by Parra Bastidas et al. (2016). For the initially dense model, the cumulative surface settlement of 0.40 m suggests a final average D_R of 99%. These average D_R values estimated from surface settlements are reasonably consistent with the values inferred from the cone data for both models (Figures 6c and 7c) considering the actual variation in D_R with depth, the uncertainty in D_R-q_{c1N} correlations, and other sources of experimental error.

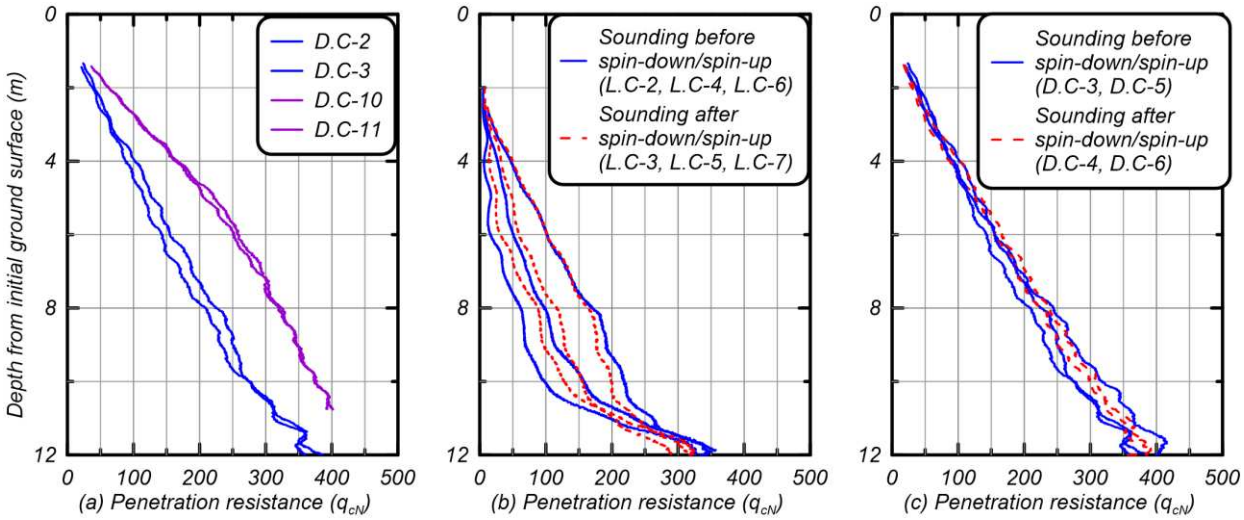

Figure 9. Cone profiles showing changes not related to shaking history.

Two pairs of cone tests in the initially dense sand model provide a basis for evaluating measurement repeatability and/or model uniformity over short distances. The cones in each pair were pushed immediately after each other (i.e. in the same centrifuge spin and without any intervening shaking event). The first pair was pushed before any shaking (D.C-2 and D.C-3), and the second pair was pushed after all shaking events (D.C-10 and D.C-11). The q_{cN} profiles from these pairs, as shown in Figure 9a, indicate that measurements were repeatable, although small differences can be expected at any given depth for locations spaced 100 mm (model scale) apart.

Several pairs of cone tests provide a basis for evaluating the effect that stopping and restarting the centrifuge (i.e. spin-down and spin-up) may have on q_{cN}. A spin-down/spin-up cycle does not measurably affect the D_R of the models (based on surface settlement measurements), but it does impose a large change in the imposed overburden stresses that may affect the coefficient of lateral earth pressure at rest (K_o) and other aspects of soil behavior that are capable of affecting cone penetration resistances (e.g. Wilson and Allmond 2014, El-Sekelly et al. 2017). The following cones were separated in time by a centrifuge spin-down/spin-up cycle without any intervening shaking event: cones L.C-2 and L.C-3, L.C-4 and L.C-5, and L.C-6 and L.C-7 in the initially loose model and cones D.C-3 and D.C-4, and D.C-5 and D.C-6 in the initially dense model. Profiles of q_{cN} for these pairs of cones are shown in Figures 9b and 9c for the initially loose and initially dense models, respectively. The differences in q_{cN} before and after a spin-down/spin-up cycle appear to be relatively small on average, with small increases and small decreases observed over different depth intervals for different pairs. Overall, any differences due to spin-down/spin-up cycles are no greater than those between successive cones located adjacent to each other without any intervening shaking or loading event (Figure 9a).

The cone data were also examined for any systematic trends in q_{cN} relative to the timing of shaking events that did and did not trigger liquefaction to different extents. No discernible patterns were identifiable that would be considered significant relative to the differences that appear attributable to local spatial variations alone.

4 CONCLUSIONS

The effect of shaking history and prior liquefaction events on cone penetration resistance was evaluated using a pair of saturated sand models, with initial relative densities of 25-30 and 75-80%, subjected to repeated shaking events on the UC Davis 9-m radius geotechnical centrifuge.

Cone penetration resistance progressively increased with successive shaking events as the model became progressively denser and more resistant to excess pore pressure generation even when subjected to relatively strong shaking intensities. For the initially loose sand model, cone penetration resistances increased almost eight-fold and relative densities increased to 80-90% over much of the layer after 24 shaking events. For the initially dense sand model, cone penetration resistances increased almost two-fold and relative densities increased to 80-100% over much of the layer after 17 shaking events. The patterns of densification with respect to depth and shaking event for the two models were shown to be consistent with pore pressure dissipation patterns during and after shaking events.

Penetration resistances in sand in the field depend on several factors that were not addressed in this study, including age and cementation. Regardless, these data suggest that the cumulative effects of multiple shaking/liquefaction events over geologic time can be expected to produce similarly large cumulative increases in penetration resistance.

5 ACKNOWLEDGMENTS

The National Science Foundation (NSF) provided the funding for this research (Grant No. CMMI-1300518) and for the Natural Hazards Engineering Research Infrastructure (NHERI) centrifuge facility at UC Davis

(Grant No. CMMI-1520581). The views and conclusions presented in this paper are the solely the authors' and do not necessarily reflect the views/opinions of NSF. This research would not have been possible without the help of Dan Wilson, Mohammad Khosravi, Ali Khosravi, Alex Strum, Bao Li Zheng, Kevin Kuei, Matt Burrall, Sean Munter, Erik Maroney, and Diane Moug. The authors would like to thank the staff and researchers at the UC Davis Center for Geotechnical Modeling for their assistance and the University of Western Australia for the CPT design.

6 REFERENCES

Bolton, M. D., Gui, M. W., Garnier, J., Corte, J. F., Bagge, G., Laue, J., and Renzi, R. 1999. Centrifuge cone penetration tests in sand. Geotechnique, 49(4), 543-552.

Darby, K. M., Bronner, J. D., Parra Bastidas, A. M., Boulanger, R. W., and DeJong, J. T. 2016. Effect of shaking history on cone penetration resistance and cyclic strength of saturated sand. Proceedings, Geotechnical and Structural Engineering Congress, ASCE, Phoenix, AZ, February 14-17.

Dobry, R., and Abdoun, T. 2016. Research findings on liquefaction triggering in sands during earthquakes. H. Bolton Seed Lecture. Geotechnical and Structural Engineering Congress, ASCE, Phoenix, AZ, February 14-17.

El-Sekelly, W., Abdoun, T., and Dobry, R. 2015. Liquefaction resistance of a silty sand deposit subjected to preshaking followed by extensive liquefaction. *Journal of Geotechnical and Geoenvironmental Engineering*, 04015101.

El-Sekelly, W., Dobry, R., Abdoun, T., and Steidl, J. H. 2016. Centrifuge modeling of the effect of preshaking on the liquefaction resistance of silty sand deposits. *Journal of Geotechnical and Geoenvironmental Engineering*, 04016012.

El-Sekelly, W., Abdoun, T., and Dobry, R. 2017. Effect of sand overconsolidation and extensive liquefaction on K0. Proceedings, Geotechnical Frontiers, ASCE, Orlando, FL, March 12-15.

Ha, I. S., Olson, S. M., Seo, M. W., and Kim, M. M. 2011. Evaluation of reliquefaction resistance using shaking table tests. *Soil Dynamics and Earthquake Engineering,* 31(4), 682-691.

Idriss, I. M., and Boulanger, R. W. 2008. *Soil liquefaction during earthquakes,* Earthquake Engineering Research Institue, Oakland, CA.

Parra Bastidas, A. M., Boulanger, R. W., Carey, T. J., DeJong, J. T. 2016. *Ottawa F-65 sand data from Ana Maria Parra Bastidas*. http.//nees.org/resources/13738.

Price, A. B., DeJong, J. T., and Boulanger, R. W. 2017. Cyclic loading response of silt with multiple loading events. *Journal of Geotechnical and Geoenvironmental Engineering, in-press*

Sharp, M. K., Dobry, R., and Phillips, R. 2010. CPT-based evaluation of liquefaction and lateral spreading in the centrifuge. *Journal of Geotechnical and Geoenvironmental Engineering,* ASCE, 136(10), 1334-1346.

Wilson, D. W. & Allmond, J. D. 2014. Advancing geotechnical earthquake engineering knowledge through centrifuge modeling. *Physical Modelling in Geotechnics- Gaudin & White (Eds). London. 125-137.*